Applied Catalysis B: Environmental 181 (2016) 550–560

Contents lists available at ScienceDirect

Applied Catalysis B: Environmental

journal homepage: www.elsevier.com/locate/apcatb

Catalytic removal of trichloroethylene from water over palladium loaded microporous and hierarchical zeolites

Anna Śrębowata[a], Karolina Tarach[b], Vladimir Girman[c], Kinga Góra-Marek[b,*]

[a] Institute of Physical Chemistry PAS, Kasprzaka 44/52, 01-224 Warsaw, Poland
[b] Faculty of Chemistry, Jagiellonian University in Kraków, 3 Ingarden Street, 30-060 Kraków, Poland
[c] Pavol Jozef Šafárik University in Košice, Department of Condensed Matter Physics, Park Angelinum 9, 041 54 Košice, Slovakia

ARTICLE INFO

Article history:
Received 30 May 2015
Received in revised form 31 July 2015
Accepted 12 August 2015
Available online 18 August 2015

Keywords:
Pd-zeolites
Hydrodechlorination
Trichloroethylene
CO sorption
IR spectroscopy

ABSTRACT

The work was aimed to investigate the catalytic properties of Pd- containing ZSM-5 zeolites in hydrodechlorination of trichloroethylene (TCE HDC) in aqueous phase. Conventional purely microporous zeolite ZSM-5 and its mesostructured analogue obtained by alkaline leaching were used as the supports for palladium moieties. The resulting materials were subjected to chemical analysis, XRD characterization, CO chemisorption, and spectroscopic investigation (XPS and FTIR) and, then, used as the catalysts in removal of trichloroethylene from drinking water. The studies have shown clearly that catalytic performance of palladium loaded materials depended on acidic and textural properties of zeolites, which influenced both noble metal dispersion and Pd^0/Pd^{2+} ratio. In a series of the zeolite catalysts the best results were obtained for palladium deposited on desilicated form of ZSM-5. Palladium in the form of uniformly dispersed species, containing large amount of Pd^0 species was found to be significantly active in TCE HDC.

1. Introduction

Although water is an essential substance for our life, the access to the clean resources becomes problematic due to e.g., a contamination of both ground and drinking water by chlorine containing volatile organic compounds (Cl-VOC's). These completely synthetic organic compounds possessing anesthetic and carcinogenic properties have been recognized as a destructive to the human liver and kidney. Due to high volatility and strong recalcitrance to degradation, chloroorganic compounds can be transported over long distances in different environment media [1]. One of the most popular Cl-VOC's is trichloroethylene (TCE). It is commercially important reagent used as end product and intermediate moiety in the manufacture of other chemicals, i.e. industrial solvents, detergents for dry cleaning; thus its elimination or finding substitute becomes impossible. Therefore, there is still an increasing need for technologies which would convert harmful (usually carcinogenic and mutagenic) chlorocarbons into environmentally benign products such as hydrocarbons [2,3]. Attractive and environmentally friendly method of removal Cl-VOC's from an environment is catalytic hydrodechlorination (HDC). It is one of the most universal resource- saving methods for reprocessing chloroorganic compounds [4] allowing re-use of the final products of the HDC process [5]. The cost of HDC would be associated mainly to hydrogen consumption and catalysts. Non-reacted hydrogen can be recirculated to the reactor after scrubbing/absorption with water or alkaline solution to remove HCl, which reduces substantially reagents costs [6,7]. Noble metals such as palladium and platinum, thanks to strong hydrogenation activity are still considered as the most popular catalyst in hydrodechlorination processes [7–9]. In addition to metal phase, the support plays an important role in both catalytic activity and stability of the catalyst. Silica, alumina and active carbons [10–12] are used as the most popular supports for dispersed metal phase. Very interesting, but still not very widely held materials are the zeolites, especially in hydrodechlorination of C_2 chlorocarbons in aqueous phase [13–19]. However, nickel–containing dealuminated zeolite BEA was found to be active and stable catalyst in HDC of 1,2-dichloroethane and trichloroethylene with very high selectivity toward value added products (unsaturated hydrocarbons). In contrast, HDC on nickel loaded conventional zeolite BEA led to strong deactivation of catalysts during reaction and provided less chlorinated hydrocarbons as major products [20–22]. Recently, zeolites have been used for the catalytic oxidation of CVOCs. The main advantages of zeolites is the presence of the micropores of molecular dimensions responsible for their extremely high surface area and shape selectivity.

* Corresponding author.
E-mail address: kinga.goramarek@gmail.com (K. Góra-Marek).

http://dx.doi.org/10.1016/j.apcatb.2015.08.025
0926-3373/

However, diffusional limitations are frequently observed especially when large molecules are processed. Thus to improve the catalyst effectiveness in chemical reactions, desilication i.e., controlled silicon extraction from the zeolite framework in alkaline aqueous solution has been developed as one of the most efficient methods to design micro- and mesoporous (hierarchical) zeolites [23–27]. Despite the fact that desilication has been successfully applied to produce a large number of hierarchically structured zeolites, the benefits of hierarchical zeolites for hydrodechlorination process have not been reported in previous studies.

Encouraged by a high effectiveness of zeolitic materials in Cl-VOC's removal from gaseous phase [20–22] we decided to investigate the applicability of Pd-loaded microporous and hierarchical ZSM-5 zeolites in hydrodechlorination of trichloroethylene in aqueous phase. Purely microporous zeolite HZSM-5 was faced with its hierarchical analogue HZSM-5/DeSi to evaluate the advantage of the presence of an additional mesopore system in catalytic performance. Both palladium loaded catalysts (marked as 0.5 wt.% Pd/HZSM-5 and 1.0 wt.% Pd/HZSM-5/DeSi) were characterized by e.g., chemical analysis, X-ray diffraction (XRD), CO chemisorption, XPS, and Fourier transformed infrared spectroscopy (FTIR) and, then were investigated as the catalysts in removal of trichloroethylene from ground and drinking water.

2. Experimental

2.1. Catalyst preparation

The parent zeolite NH_4ZSM-5 of molar ratio Si/Al = 32 was purchased from Zeolyst (CBV5524G), the particle size diameter is 200–300 nm. Desilication was carried out in the 0.2 M NaOH solution at the temperature of 65 °C for 0.5 h. After desilication, the suspension was cooled down in ice-bath, filtered, washed with distillate water until neutral pH was reached, and dried at room temperature. Next three-fold ion-exchange procedure with 0.5 M NH_4NO_3 at 60 °C was applied to obtain NH_4-form of both microporous and mesostructured zeolites. After ion-exchange zeolites were filtered, washed with distilled water, dried at 110 °C and calcined at 500 °C.

The synthesis of catalysts containing palladium with the use of aqueous solution of 2.5×10^{-3} M $PdCl_2$ was conducted basing on the methods described in refs [28,29]. The pH of solutions was kept in the range of 3–4 by addition of suitable amounts of a HCl solution (0.1 M). The molar ratio of $PdCl_2$:HCl was 1:5. The synthesis of catalysts was conducted as follows: to specified volume of $PdCl_2$ solution an appropriate amount of zeolites HZSM-5 and HZSM-5/DeSi was added, and the obtained suspension was stirred at room temperature until the complete adsorption of Pd^{2+} ions. Completeness of adsorption was colorimetric monitored by the reaction with thiourea. Then, the solid was filtered and washed with distilled water until Cl^- ions were absent in a filtrate. Finally, the samples were dried at room temperature. Detailed conditions of the impregnation procedure of HZSM-5 zeolite are given in the Table 1. Solutions of precursor were prepared in-situ. Time necessary to complete adsorption of Pd^{2+} ions was 36 h.

2.2. Characterization of the catalysts

2.2.1. Structural and textural properties: ICP, XRD and N_2 low temperature sorption studies

Si and Al content in the parent and desilicated zeolites was determined by ICP OES spectroscopy on an Optima 2100DV (PerkinElmer) instrument.

Pd content was determined by ICP AES analysis (Table 1) using a high-performance sequential plasma spectrometer (Model ARL 3410 ICP). Palladium was marked at wave lengths of 360.955 and 340.458 nm. The solid samples were digested (in a mixture of HF, HCl and HNO_3) in a microwave oven for special temperature program. Then, aliquots of solution were diluted to a volume of 100 ml using deionized water. The Pd content in the resulting samples was established to be equal of 0.5–1.0 wt.%. The sample codes include information about the Pd loading.

The BET surface area and pore volume of the samples were determined by N_2 sorption at −196 °C using a 3Flex (Micromeritics) automated gas adsorption system. Prior to the analysis, the samples were degassed under vacuum at 250 °C for 24 h. The specific surface area (S_{BET}) was determined using BET (Brunauer–Emmett–Teller) model according to Rouquerol recommendations [30]. The micropore volume and specific surface area of micropores were calculated using the Harkins-Jura model (*t*- plot analysis).

The X-ray diffraction (XRD) patterns of the samples were recorded with a D2 Phaser diffractometer (Bruker) using Cu Kα radiation (λ = 1.54060 Å, 30 kV, 10 mA).

2.2.2. IR spectroscopy studies with probe molecules

Prior to FTIR studies, all samples were pressed into the form of self- supporting discs (ca. 5 mg/cm^2) and in-situ thermally treated in an IR cell at 550 °C under vacuum for 1 h.

Sorption of pyridine (Py) (Avantor Performance Materials Poland S.A., 99.9%) and carbon monoxide (Linde Gas Poland 99.5%) were performed on the vacuum pre-treated samples. Sorption of CO was performed at −100 °C, while for Py sorption the standard quantitative procedure was applied [26,27]. Sorption of 1,1,2-trichloroethylene (TCE, Sigma–Aldrich, ≥99.5 %) was carried out at room temperature.

Spectra were recorded with a Bruker Tensor 27 spectrometer equipped with an MCT detector. The spectral resolution was of 2 cm^{-1}. All IR spectra presented in this work were normalized to the same mass of sample (10 mg).

2.2.3. CO chemisorption studies

The samples were investigated by chemisorption measurement in a static system. CO adsorption was measured at 35 °C, using a backsorption method with an ASAP 2020Chem instrument from Micromeritics. Before collecting the adsorption isotherms palladium catalysts were reduced at 380 °C for 3 h, and next cooled down to CO adsorption temperature.

2.2.4. XPS studies

The X-ray photoelectron spectra (XPS) were measured on a Prevac photoelectron spectrometer equipped with a hemispherical VG SCIENTA R3000 analyser. The photoelectron spectra were measured using a monochromatized aluminium Al Kα source(E = 1486.6 eV) and a low-energy electron flood gun (FS40A-PS) to compensate the charge on the surface of nonconductive samples. The base pressure in the analysis chamber during the measurements was 5×10^{-9} m bar. Spectra were recorded with constant pass energy of 100 eV for the survey and for high-resolution spectra. The binding energy scale was referenced to the Au 4f7/2peak (84.0 eV) of a clean gold. The composition and chemical surrounding of the sample surface were investigated on the basis of the areas and binding energies of Pd 3d, Al 2p, Si 2p and O 1s photoelectronpeaks. The fitting of high-resolution spectra was provided through the CasaXPS software when a Shirley background was used. A mixed Gaussian–Lorentzian function was used to describe the peak shape.

2.2.5. STEM studies

The micrographs were obtained using transmission electron microscope (JEOL 2100F) working at 200 KV, with Field Emission

Table 1
Conditions of Pd ion-exchange for studied zeolites HZSM-5 and results of chemical analysis.

zeolite	Pd content [μmol/g]	$VPdCl_2$ [cm^3]	support mass [g]	time of exchange [h]
HZSM-5	0	–	–	–
0.5wt.% Pd/HZSM-5	50	22.0	1.00	36
1.0wt.% Pd/HZSM-5	100	44.0	1.00	36
HZSM-5/DeSi	0	–	–	–
0.5wt.% Pd/HZSM-5/DeSi	50	22.0	1.00	36
1.0wt.% Pd/HZSM-5/DeSi	100	44.0	1.00	36

Gun (FEG), EDX analysis and STEM detectors for bright and dark mode.

2.3. Catalytic tests

Catalytic tests in aqueous phase were performed at room temperature (~25 °C) and atmospheric pressure, under continuous magnetic stirring (1000 rpm), in a 500 ml round bottomed flask equipped with the pH-meter, using 350 ml MiliPore water and 20 μL of trichloroethylene. Before adding the substrate, the water had been saturated with hydrogen for 30 min, and then 0.05 g of the catalyst was added to reaction mixture. Approximately 2.5 ml of samples were periodically taken from the reactor at specified times and filtered through 0.2m, 25 mm nylon filter order to remove catalyst particles before chromatographic analysis. The samples for analysis were taken at 2, 5, 10, 15, 20, 60, 90, 120 and 150 min. The trichloroethylene concentration and products were monitored using gas chromatography system (Bruker 456-GC with ECD and FID, Headspace SHS-40). The controlled experiments without the catalysts were performed and named as the blank experiments in Section 3.4. The experiments with the supports (zeolites: HZSM-5 and HZSM-5/DeSi) have shown adsorption of chloroorganic compound on zeolite materials (results presented in Section 3.4). All of the spent catalysts after filtration, washing with distilled water and drying in the oven at temperature 120 °C were weighed. An only negligible mass lost for catalysts after reaction had been observed. Additionally, the 1.0 wt.% Pd/HZSM- 5/DeSi sample was recovered by filtration and then washed with distilled water and dried in the oven at temperature 120 °C for the subsequent catalytic run. The catalytic procedure was repeated 3 times.

3. Results and discussion

3.1. Physicochemical properties of the catalysts

Fig. 1 depicts the XRD patterns of native HZSM-5 and HZSM-5/DeSi as well as their Pd-analogues. The reflections typical of the MFI structure of almost identical intensities comparing to native zeolites can be identified in diffractograms of Pd-modified HZSM-5 and HZSM-5/DeSi. It indicates that neither desilication nor impregnation procedures disturbed the zeolitic structure. The reflections characteristic of PdO species were not identified in the diffractograms of the Pd-catalysts. While palladium species reflections cannot be discriminated from the zeolite pattern [31], their growth has been restricted by the 10-membered pores of zeolite ZSM-5, and thus they are believed to be of a small particle size. Finally, a potential ability of zeolites to inhibit active palladium particles growth and aggregation in the pores of zeolitic structure offers these structures to be ones of the best supports for Pd-loaded catalysts.

Textural parameters of the zeolitic supports and their Pd-modifications are listed in the Table 2. The NaOH leaching of zeolite HZSM-5 resulted in the extraction of Si atoms, thus the decrease of Si/Al for zeolite HZSM-5/DeSi was observed. The Pd-impregnation on zeolites HZSM-5 and HZSM-5/DeSi was also reflected in alternation of the textural parameters of both supports. The specific surface areas showed a decline with increasing palladium content for studied catalysts. A significant drop of the specific surface area followed by the decline of micropore surface and micropore volume was evidenced for purely microporous 1.0 wt.% Pd/HZSM-5 due to the location of Pd- species in micropores and finally their plaguing. The parameters describing micropore properties i.e. volume and surface of micropores were less affected by noble metal deposition in zeolite with secondary system of mesopores. An enhanced mesopore surface of HZSM-5/DeSi support was beneficial to the active phase dispersion. Indeed, CO chemisorption measurement confirmed that higher dispersion of noble metal clusters was achieved for desilicated zeolite HZSM-5/DeSi. Although, both 0.5 wt.%Pd/HZSM-5/DeSi and 1.0 wt.%Pd/HZSM-5/DeSi were treated in hydrogen flow in the temperature 380 °C, rather high palladium dispersion and the same small palladium nanoparticles size were determined: ~56% for 0.5 wt.% Pd/HZSM-5/DeSi and ~44% for 1.0 wt.%Pd/HZSM-5/DeSi, which corresponding to palladium nanoparticles size 2.01 nm and 2.57 nm, respectively. For microporous HZSM-5 zeolite palladium dispersion were smaller: ~37% for 0.5 wt.% Pd/HZSM-5 and 33% for 1.0 wt.%Pd/HZSM-5. An average size of Pd particle was found to be bigger: 3.01 nm and 3.40 nm for 0.5 and 1.0 wt.% Pd content, respectively. Additionally, as will be presented in Section 3.2.1., more pronounced Brønsted acidity of mesoporous HZSM-5/DeSi support could also influenced the active phase dispersion. Okumura et al. and Muto et al. [32,33] evidenced that the acidic properties of the support offers a higher dispersion of Pd moieties.

3.2. IR studies

3.2.1. IR quantitative studies

Pyridine (Py) molecule is widely used as a probe for quantification of both Brønsted and Lewis sites in solid catalysts [34]. Interaction of Py with acid sites resulted in the development of the 1445 cm^{-1} and 1545 cm^{-1} bands, attributed to Py-Lewis (PyL) adducts and pyridinium ions PyH^+, respectively. The concentrations of both Brønsted (PyH^+) and Lewis (PyL) acid sites in studied catalysts were calculated on the bases of the maximum intensities of the PyH^+ and PyL bands and corresponding the extinction coefficient values [35].

Concentration of Brønsted and Lewis acid sites in zeolite HZSM-5 and HZSM-5/DeSi as well as in their Pd-modified forms are presented in the Table 3. The enhanced Brønsted acidity for desilicated zeolite results from the extraction of Si atoms during alkaline treatment, thus the decrease of Si/Al ratio. The Lewis acid sites in both zeolitic supports are extraframework aluminium species (30 $\mu molg^{-1}$) which mainly originate from imperfect zeolite structure. Alkaline leaching results in an additional extraction of some aluminium atoms from the framework into extraframework positions (Al_{EXFRAM}), thus a higher contribution of Lewis acid sites (220 $\mu molg^{-1}$) was evidenced for meso/microporous material HZSM-5/DeSi. Upon deposition of Pd on both zeolites the Lewis acid centers contribution slightly increased therefore the concentration of Pd species deposited was assumed to correspond

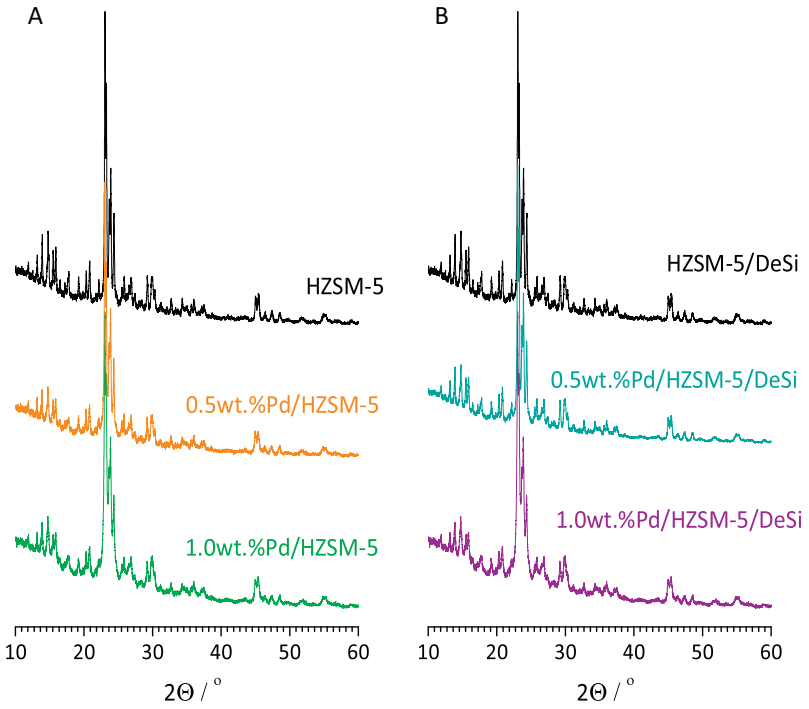

Fig. 1. XRD patterns of H and Pd-form of microporous (A) and hierarchical (B) zeolites ZSM-5.

the enhanced Lewis acidity in Pd-modified zeolites. Contribution of Pd centers accessible for reagent molecules in the catalytic process, i.e. the dispersion of Pd species, was derived from the comparison of the surface concentration of Pd centers (in μmol/g) determined in quantitative measurements of pyridine sorption and the total Pd concentration obtained from chemical analysis (Fig. 2). This anticipation on noble metal deposition is fully justified if the generation of Lewis sites others than those originating from Pd-moieties has been excluded. Apart from Pd deposition, the only factor influencing the Lewis sites concentration would be dealumination which underwent in the presence of HCl solution during Pd-deposition procedure. However, high Si/Al ratios of zeolites HZSM-5 and HZSM-5/DeSi guarantee their high resistance against dealumination. Accordingly, the number of Lewis sites attributed to Pd species can be estimated as the difference of Lewis sites present in Pd-modified zeolites and non-modified

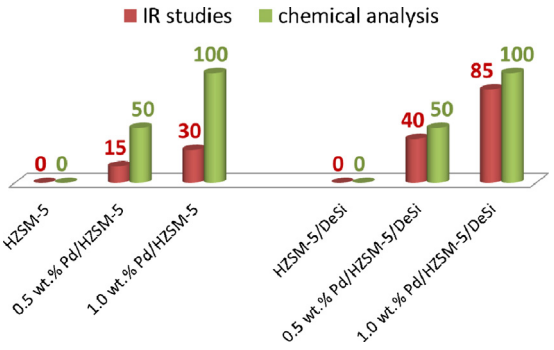

Fig. 2. Comparison of the concentration of Pd centers (in μmol/g) derived from IR experiments of Py-sorption and chemical analysis for microporous HZSM-5 and meso/microporous HZSM-5/DeSi modified with different Pd content.

Table 2
Composition (Si/Al) and textural parameters of studied zeolites.

zeolite	Si/Al	V_{micro} [cm^3/g]	V_{meso} [cm^3/g]	S_{BET} [m^2/g]	S_{micro} [m^2/g]	S_{meso} [m^2/g]
HZSM-5	32	0.17	0.06	367	327	40
0.5wt.% Pd/HZSM-5		0.15	0.06	310	273	37
1.0wt.% Pd/HZSM-5		0.10	0.05	240	220	20
HZSM-5/DeSi	20	0.16	0.28	450	305	145
0.5wt.% Pd/HZSM-5/DeSi		0.16	0.27	412	272	140
1.0wt.% Pd/HZSM-5/DeSi		0.15	0.20	399	274	125

Table 3
The composition of the parent (HZSM-5) and desilicated (HZSM-5/DeSi) zeolites determined by chemical analysis (Si/Al and Pd concentration in μmol/g) and the concentration of Brønsted (C_B) and Lewis (C_L) acid sites (in μmol/g) as well as Pd species determined in quantitative IR studies of pyridine sorption.

Zeolite	Si/Al	C_B	C_L	Pd/ICP	Pd/IR
HZSM-5	32	450	30	0	0
0.5wt.% Pd/HZSM-5		420	45	50	15
1.0wt.% Pd/HZSM-5		350	60	100	30
HZSM-5/DeSi	20	650	220	0	0
0.5wt.% Pd/HZSM-5/DeSi		640	260	50	40
1.0wt.% Pd/HZSM-5/DeSi		615	305	100	85

materials. The agreement between values derived from the chemical analysis and IR measurements for meso/microporous zeolite HZSM-5/DeSi clearly evidences very high dispersion of Pd-forms deposited on meso/microporous support (Fig. 2). For solely microporous zeolite HZSM-5 a decline in the quantities of Pd-centers detected with pyridine molecule is observed: the number of available Pd- centers provides 30% of all possible adsorption centers. This inconsistency points to the formation of palladium agglomerates which are responsible for the significant drop of micropore volume detected for zeolite HZSM-5 upon a deposition of noble metal (Section 3.1).

Also, the STEM micrographs and Pd-particle size distributions (Fig. 3) indicate that the extent of agglomeration of Pd species is different for both supports. The enhancement of mesopore surface area observed for HZSM-5/DeSi support found to be beneficial to the active phase dispersion. Indeed, the Pd deposition on hierarchical zeolite HZSM-5/DeSi is more uniform and the particles of lower than 2 nm size are evidenced in majority, with 1.7 nm of average size of Pd particles. A noble metal deposition on the solely microporous HZSM-5 results in the formation of lower dispersion agglomerates with average size of 2.2 nm. These results are in agreement with IR studies of pyridine sorption (Table 2 and Fig. 3), which also demonstrated higher accessibility of palladium species in case of hierarchical supports. Thus, it can be anticipated that higher dispersion of noble metal particles observed for meso/microporous supports will be reflected in their higher catalytic activity. It is well recognized that the size of the cluster is determined by the size of the zeolite cavity and is almost independent of either the initial form of palladium or of the cluster formation conditions [36].

3.2.2. Nature of Pd species—carbon monoxide sorption

To elucidate the nature of electron donor palladium species, carbon monoxide was employed a probe molecule. The IR spectra recorded at −100 °C after the saturation of all palladium species with CO are presented in Fig. 4. The 2125 cm^{-1} band has been attributed to CO engaged into interaction with Pd^{n+} ions in oxide forms. The development of the 2100–2000 cm^{-1} bands results from the interaction of carbon monoxide with metallic Pd^0, namely linear $Pd^0(CO)$ carbonyls [37]. The feature at 1975 cm^{-1} originates from $Pd^0{}_2(CO)_2$ adducts [38], while broad bands of the lowest frequencies. i.e., at 1945 and 1920 cm^{-1} have been assigned to the bridged carbonyls on Pd metallic species [39]. The band at 2175 cm^{-1} originates from CO hydrogen bonded to Brønsted sites, i.e., to the bridging hydroxyls Si(OH)Al.

The integral intensities of the palladium carbonyl bands were taken as measure of Pd species dispersion. It is clearly evidenced that the number of noble metal species able to bond CO molecules is greater for the Pd-catalysts based on meso/microporous zeolite HZSM-5/DeSi, than for microporous HZSM-5. Lower number of Pd species detected with CO in HZSM-5 results from the agglomeration of Pd species and can be associated with microporous character of the support. In the latter case, the pore mouths can be blocked by noble metal agglomerates, thus Pd-species hidden inside micropore are hardly accessible for CO molecules. This phenomenon is clearly evident for microporous support with the higher amount Pd deposited, 1.0 wt.% Pd/HZSM-5, being in line with a vital drop of micropore volume.

The opposite effect is observed for hierarchical zeolite HZSM-5/DeSi. The intensities of all bands ascribed to the presence of Pd forms increase with the amount of Pd deposited. The presence of secondary system of mesopores, and, in consequence, the increase of mesopore surface is believed to be responsible for a higher dispersion/accessibility of Pd species in hierarchical zeolite HZSM-5/DeSi. Interestingly, in comparison with 0.5 wt.% Pd/HZSM-5/DeSi, the predominant carbonyl species developed in hierarchical zeolite with 1.0 wt.% Pd are the bridged Pd carbonyls. It has been reported that the monocarbonyls are formed on isolated metallic species while the bridged carbonyls are mainly formed on agglomerated metallic moieties [40,41]. Indeed, the CO chemisorption data pointed to the presence of palladium nanoparticles of bigger average diameter (2.57 nm) in 1.0 wt.%/Pd/HZSM- 5/DeSi than in catalyst with lower Pd content (2.01 nm). On the other hand, Pd particle diameter distribution derived from STEM studies evidenced a significantly higher dispersion of Pd-nanoparticles (1.7 nm average nanoparticle diameter) in zeolite with bigger Pd content, 1.0 wt.% Pd/HZSM- 5/DeSi. Thus, the coexistence of highly dispersed Pd particles (evidenced by STEM studies) and more aggregated species (IR studies of CO sorption) cannot be excluded in 1.0 wt.% Pd/HZSM-5/DeSi. Finally, it is clearly seen that only comprehensive evaluation of active species dispersion with use of several different methods will give real insight into catalyst surface.

3.2.3. Sorption of 1,1,2-trichloroethylene

Interaction of TCE molecules with the catalyst surface was examined with IR spectroscopy both for purely microporous and hierarchical zeolites. As an example the IR spectra collected for 1.0 wt.%. Pd HZSM-5/DeSi saturated with TCE are presented in Fig. 5. Scrutiny of the IR spectra revealed that TCE molecules are hydrogen bonded to acidic bridging Si(OH)Al groups which is detected as the minimum at the position of the 3610 cm^{-1} Si(OH)Al band. The 3099 cm^{-1} band, attributed to stretching C—H vibrations confirms the presence of TCE adsorbed on zeolite surface—spectrum a. Introduction of H_2 over catalyst did not influence TCE adsorbed species (spectrum not shown). Nevertheless, after 30 min. contact time of reagents with zeolite the 3099 cm^{-1} TCE band started to be consumed, while new sharp bands in the 3000–2600 cm^{-1} frequency region appeared. The rise of reaction temperature to 50 °C increased the reaction rate and after 120 min. all TCE molecules were transformed in hydrodechlorination products—spectrum d. Among them HCl, ethane, and ethene can be easily recognized in IR spectrum by comparison with the reference spectra (e.g). Neither vinyl chloride, 1,1-dichloroethylene nor *cis*-and *trans*-dichloroethylene were identified in our IR spectra (spectra c-d), however if yes, they were formed only in trace amounts. Indeed, the product ratios formed during the dehalogenation reaction have been found to be dependent on the metal speciation and the concentration of hydrogen in the aqueous phase [42,43].

The relative activity of studied catalysts was estimated by the comparison of the intensity of the product dehalogenation bands after 30 min. of reaction at 50 °C (Fig. 6). The bands of unreacted TCE (3099 cm^{-1}) was present only for purely microporous zeolites independently from Pd loading. The dehalogenation reaction was more facilitated for zeolites with secondary system of mesopores, the TCE band at 3099 cm^{-1} disappeared confirming the transformation of all TCE molecules in dehalogenation products. Consequently, the higher Pd loading the higher intensity of the reaction product bands were observed.

Catalytic performance of Pd-catalysts was also investigated in the presence of adsorbed water molecules. Interestingly, the water molecules were preferably bonded to the Si (OH) Al groups while Pd species have remained saturated with TCE molecules: the intensities of TCE bands at 1586 and 3092 cm^{-1} were not perturbed by the presence of water molecules (Figs. 7A and B, spectra b-c). Simultaneously, water molecules were engaged into the interaction with bridging hydroxyls what was detected as the negative band at 3614 cm^{-1} (Fig. 7A, spectrum c). The presence of water was confirmed also by a broad band at 1624 cm^{-1} (Fig. 7B, spectrum c). Again HCl, ethane, and ethene were detected as reaction products in the spectrum tracked after 120 min. contact time at 50 °C of H_2O/TCE/H_2 over 1.0 wt.% Pd/HZSM-5/DeSi (Fig. 7, spectrum d).

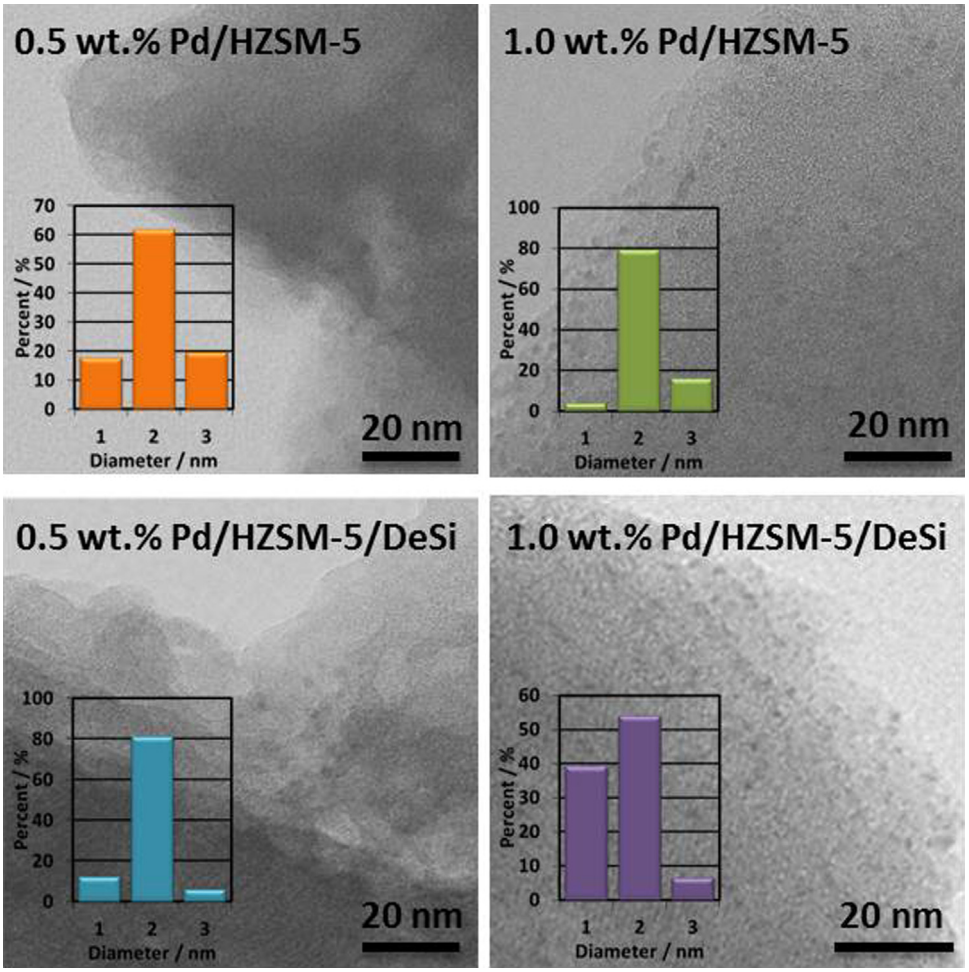

Fig. 3. STEM microphotographs of the HZSM-5 and HZSM-5/DeSi with deposited palladium (20 nm). Particle diameter distribution in the form of a histogram of Pd nanoparticles.

This demonstrates that the presence of water did not affected the catalytic behaviour of studied catalyst.

3.3. XPS studies

X-ray photoelectron spectroscopy was applied to differentiate catalytic behaviour of Pd species dispersed on studied zeolites. The Si 2p, Al 2p, O 1s peaks of both supports (HZSM-5 and HZSM-5/DeSi) have been characterised by the same binding energy and intensity ratios for all the studied catalysts.

Fig. 8 depicts the XPS spectra of Pd-zeolites and the measured binding energies are gathered in the Table 4. The peaks attributed to Pd^{2+} $3d_{3/2}$ and Pd^{2+} $3d_{5/2}$ fit well with PdO, while the larger peaks of lower binding energies correspond to pure metallic Pd (Pd^0 $3d_{3/2}$ and Pd^0 $3d_{5/2}$) [44–46].

The values of binding energies evidences a shift for both $Pd^0{}_{3d}$ (0.5–1.0 eV) and $Pd^{2+}{}_{3d}$ (0.4–0.6 eV) when the support changes

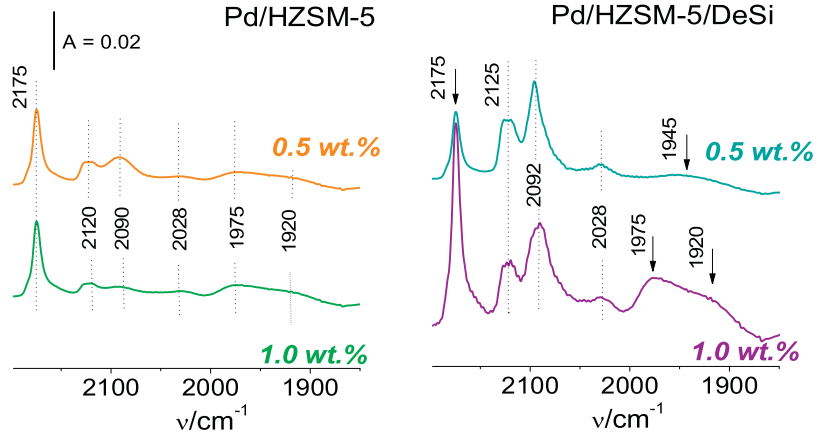

Fig. 4. IR spectra of CO (carbonyl species frequency region) adsorbed on studied Pd-zeolites.

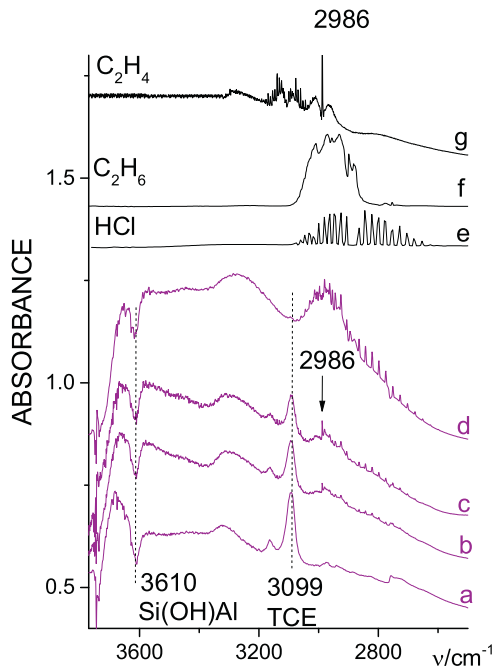

Fig. 5. IR spectra of TCE adsorbed on HZSM-5/DeSi with 1.0 wt.% Pd deposited and the products of it transformation in the presence of hydrogen.
a – Spectrum recorded at RT after TCE and H_2 sorption (TCE:H_2 = 1:2); b – spectrum recorded at RT after 30 min. contact time of reagents with zeolite; c – spectrum recorded at RT after 5 min contact time at 50 °C; d – spectrum recorded at RT after 30 min contact time at 50 °C; reference spectra: gaseous HCl (e), ethane (f), ethene (g).

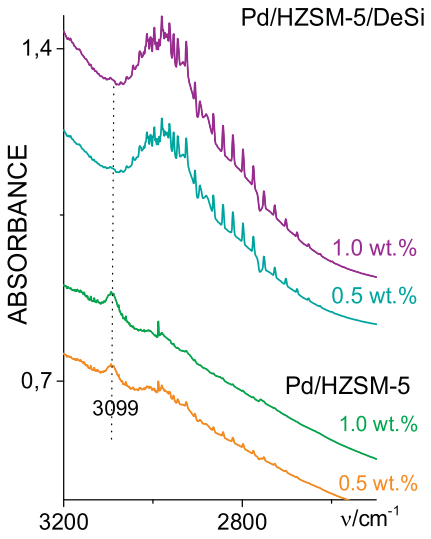

Fig. 6. IR spectra of collected after TCE transformation at 50 °C for 30 min.

from purely microporous (HZSM-5) to micro/mesoporous one (HZSM-5/DeSi)—Table 4. The most likely, the change of the binding energy results from the interaction of the Pd species with the HZSM-5/DeSi support of acidic properties more pronounced than those of HZSM-5. Thus metal moieties appear to be electron deficient in desilicated zeolite. Also the distribution of Pd species between Pd^{2+} and Pd^0 strongly depended on the type of zeolitic support. The Pd^{2+}/Pd^0 values derived from XPS spectra pointed to bigger amount of metallic palladium hosted in hierarchical zeolite. This observation supports the results of CO sorption IR experiments (Section 3.2.2).

The changes in the Pd particle size were also reflected in the values of binding energy; the Pd particles of the lower dispersion in microporous HZSM-5 are characterized by lower values of the binding energy. The confirmation of increasing size of noble metal particles was provided by STEM studies and quantitative IR investigations. Consequently, it can be anticipated that lowered activity observed for microporous zeolite HZSM-5 can be related to the formation of less dispersed, thus less active forms of Pd species.

3.4. Catalytic activity

To eliminate the effect of organic solvent on HDC rate and products distributions, the catalytic removal of trichloroethylene from water was performed without additional organic chemicals. The Fig. 9 shows the TCE conversion expressed as C/C_0 versus time of reaction carried out in the presence of H-zeolites (HZSM-5 and HZSM-5/DeSi) and palladium loaded zeolites. In accordance with previous studies on the use of zeolites in the wastewater treatment [47,48], both of protonic forms have shown a comparable efficiency of trichloroethylene adsorption from water after 150 min. The results derived from chromatographic analysis of the reaction mixture showed only the loss of TCE amounts in water, however, without formation of any hydrodechlorination products. High specific surface area and the presence of micro- and mesopores organized in a characteristic channel structure (Table 2) could play the crucial role only in adsorption capacity of both H-zeolites. The disturbance of the adsorption profile for HZSM-5 in contrast to HZSM-5/DeSi (Fig. 9) being observed as the gradual depletion of the TCE in the solution during the first 60 min and then increasing of the concentration of the reactant, could be explained by diffusional problems characteristic for purely microporous materials [13,35]. Besides various pore hierarchies, H-zeolites were characterized by different concentrations of Brønsted and Lewis acid sites (Table 3). Nevertheless, similar amounts of adsorbed TCE for HZSM-5 and HZSM-5/DeSi after 150 min of the process (Fig. 9) could suggest an insignificant role both porosity and the acid sites concentration in this process.

Introduction of small amounts of palladium (0.5 and 1.0 %wt., respectively) to HZSM-5 and HZSM-5/DeSi significantly increased

Table 4
XPS binding energy peak positions in studied Pd-zeolites.

Peak	Binding energy [eV]			
	HZSM-5		HZSM-5/DeSi	
	0.5wt.% Pd	1.0wt.% Pd	0.5wt.% Pd	1.0wt.% Pd
Pd^0 $3d_{3/2}$	339.7	340.2	340.7	340.7
Pd^0 $3d_{5/2}$	334.8	335.0	335.6	335.3
Pd^{2+} $3d_{3/2}$	341.1	341.8	341.9	342.0
Pd^{2+} $3d_{5/2}$	335.9	336.4	337.0	336.8
Pd^{2+}/Pd^0	1.3: 1.0	1.1: 1.0	1.0: 1.0	0.88: 1

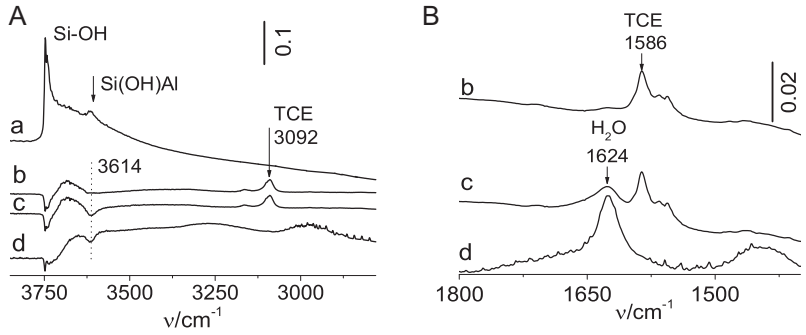

Fig. 7. IR spectra in the O—H and C—H stretching (A) and deformation (B) vibrations region recorded at room temperature for 1.0 wt.% Pd/HZSM-5/DeSi.
a – Activated sample; b – after TCE adsorption; c – after TCE and H_2O coadsorption (TCE:H_2O = 1:2); d – after introduction of H_2 (TCE:H_2 = 1:2) and 120 min. Contact time at 50 °C.

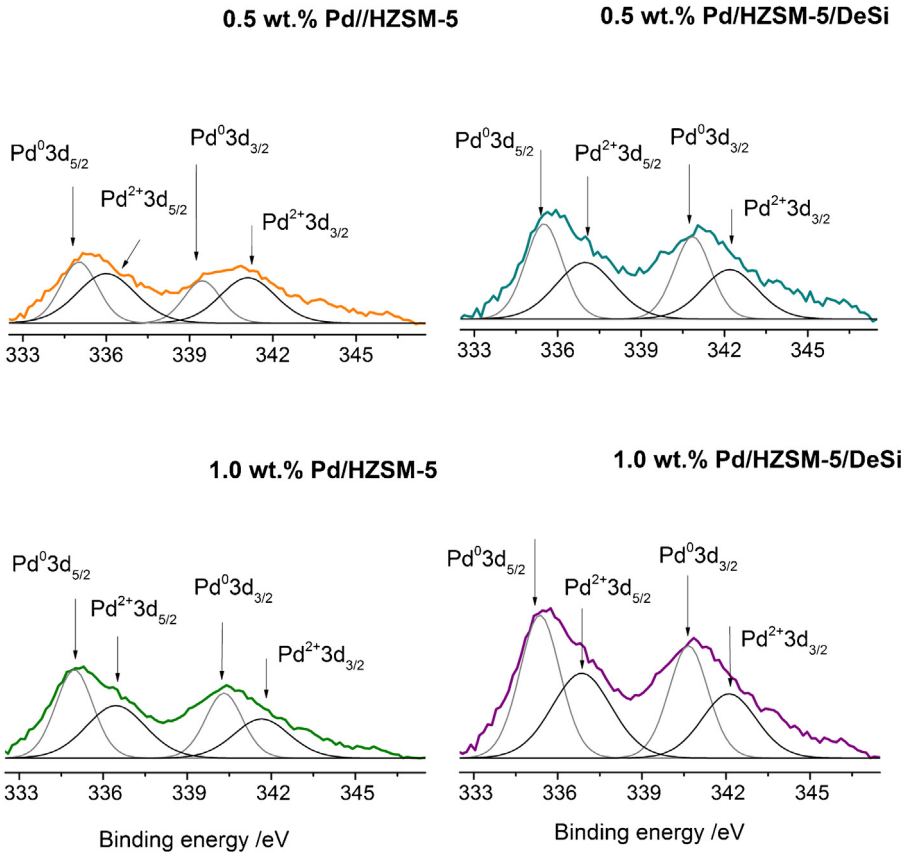

Fig. 8. XPS spectra of studied zeolites.

productivity of TCE hydrodechlorination. Both the presence of 100% of hydrocarbons (mainly ethane) as reaction products and the decreasing of pH value during the time indicated that hydrodechlorination process has occurred (Table 5). A comparative study between as prepared microporous 0.5 wt.% and 1.0 wt.%Pd/HZSM-5 as well as hierarchical 0.5 wt.% and 1 wt.%Pd/HZSM-5/DeSi have shown similar profiles C/C_0 within both series (Fig. 9C); nevertheless the catalysts with lower Pd loading have shown lower activities

Table 5
The reaction rate constant k, initial reaction rate, TOF values and selectivity towards products for hydrodechlorination of trichloroethylene on palladium loaded zeolites.

Catalyst	Initial rate r (mmol min^{-1} g^{-1}_{Pd})	TOF[a] (s^{-1}) × 10^{-2}	Selectivity (%)	
			C_2H_4	C_2H_6
0.5wt.%Pd/HZSM-5	24.40	11.68	4.5	95.5
1.0wt.%Pd/HZSM-5	7.66	4.10	3.0	97.0
0.5wt.%Pd/HZSM-5/DeSi	52.66	16.67	1.2	98.8
1.0wt.%Pd/HZSM-5/DeSi	40.92	16.49	1.3	98.7

[a] TOF calculated using the formula TOF (s^{-1}) = $r0 \times M \times 10^{-3} \times 100 \times 1/D \times 1.60$, where r_0(mmol min^{-1} g^{-1}_{Pd}) represents initial rate, M (g mol^{-1})–the atomic mass of Pd and D(%)–metal dispersion [54].

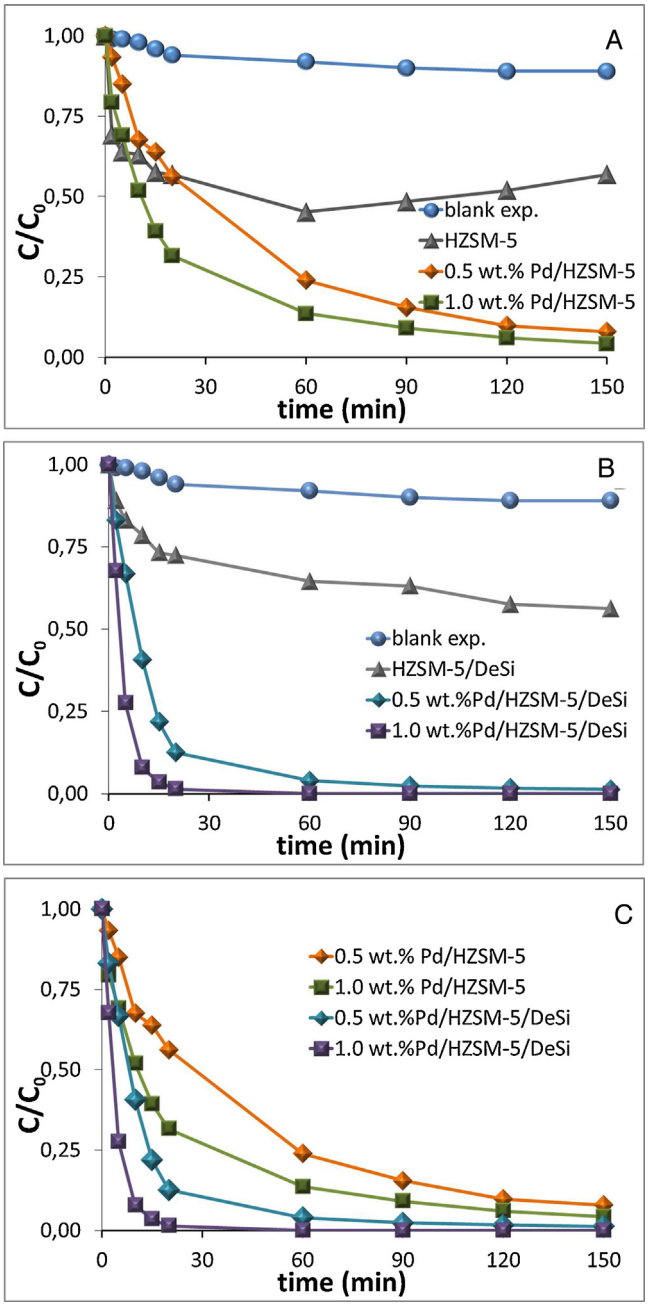

Fig. 9. Kinetics of TCE hydrodechlorination in the presence of (A) microporous HZSM-5 and Pd/HZSM-5 catalysts and (B) meso/microporous HZSM-5/DeSi and Pd/HZSM-5/DeSi catalysts. Comparative results obtained for HDC TCE on palladium containing zeolites (C).

as C/C_0 in comparison with 1.0wt% Pd loaded catalysts. Due to the lack of the significant differences in the catalytic performance of both H-zeolites, the palladium loading and metal dispersion are believed to play the crucial role in catalytic behaviour of Pd/HZSM-5 and Pd/HZSM-5/DeSi in hydrodechlorination of trichloroethylene in aqueous phase. The application of the micro/mesoporous HZSM-5/DeSi as the active support material for noble metal phase led to the formation of uniformly dispersed palladium species, what has been confirmed both in CO chemisorption and STEM studies. The average Pd particles size less than 2 nm for HZSM-5/DeSi samples can be assigned to higher activity in TCE HDC than this observed for analogous palladium species accommodated in microporous HZSM-5 (Table 3, Fig. 8C). The use of 50 mg of 1.0 wt.%Pd/HZSM-5/DeSi catalyst with the highest dispersion of metallic phase led to removal more than 90% of TCE after the first ten minutes of the reaction.

Generally, noble metal dispersion strongly influences hydrodechlorination effect, but there is no general rule for the structural sensitivity of metallic phase in HDC in both gas and water phase. Therefore this issue is still very controversial. It has been stated that an increase of the particles size leads to increase of HDC rate, both in gas and in liquid phase [48–51]. Authors explain this phenomenon by their higher resistance to HCl, however Janiak et al. [52] showed that larger palladium particles are more susceptible to leaching. Carbon materials due to their high adsorption capacity for organic compounds and high stability under the aggressive conditions of the reaction play very important role as the supports for active phase in purification of water from chloroorganic compounds [51]. Activated carbon, carbon nanofiber, or high surface area graphite with different Pd nanoparticles size were considered as the supports for palladium. The results of aqueous phase trichloroethylene hydrodechlorination preformed over carbonaceous catalysts clearly indicated that this reaction is structure sensitive, and the largest palladium particles were the most active for this reaction under the studies conditions [51] . Diaz et al. [51] have also reported that the chemistry of the supports seems to play a less determinant role in liquid-phase HDC reactions than in gas-phase reactions. On the other hand, several authors have reported a beneficial role of the small Pd-particles on overall activity metallic catalysts [20,53]. Hydrodechlorination of TCE on 0.5 wt.% Pd supported on different materials, such as: activated carbon, carbon nanofibers, high surface area graphites, alumina and ZSM-5 zeolite, showed the best results for catalysts with the higher palladium dispersion [13]. Also the studies of pillared clays supported Pt, Pd and Rh catalysts with different metal dispersion in hydrodechlorination of chlorophenols [54] led to the conclusion that the highest dechlorination activity towards environmentally friendly product – cyclohexanol- was achieved for the catalysts with the highest metal dispersion. Recent works of Dong et al. [55,56] concerning aqueous phase hydrodechlorination of 4-chlorophenol on Au and Pd nanoparticles supported on magnetic porous carbon (MPC) composite [55], and novel fibrous nano-silica based Ni@Pd core–shell nanoparticles [56] also showed beneficial role of excellent dispersed metallic phase in efficient hydrodechlorination of chloroorganic compounds. Moreover, application these new, unconventional supports prevents agglomeration of active phase, its deactivation and leaching [49–55]. Aramendia et al. [49], studying bromobenzene hydrodebromination, suggested significant role of the electronic factors in overall activity considering small Pd clusters more electro-deficient than large crystallites. Gómez-Quero et al. [57] pointed out the smallest particles (lower than 5 nm) as the most active in the hydrodechlorination of 2,4-dichlorophenol on Pd/Al_2O_3 catalyst. Also our results obtained for Pd containing zeolites HZSM-5 and HZSM-5/DeSi pointed to the beneficial role of an excellent dispersion of palladium species in hydrodechlorination of TCE.

Activity of palladium containing zeolites could depend on the Pd^0/Pd^{2+} ratio, especially in the initial time of the reaction. The IR studies of CO sorption on both Pd-catalysts have shown the presence of predominantly amounts of Pd^0 forms for Pd/ HZSM-5/DeSi. According to Ordonez et al. [58] there is a correlation between the increase in concentration of Pd^{2+} and the activity loss. Indeed the largest amounts of Pd^0 species in Pd/ HZSM-5/DeSi provoked the highest activity of this catalyst in TCE HDC. Higher activity of Pd^0 containing HZSM-5/DeSi could also depend on spill- over of hydrogen atoms from palladium to the support. Furthermore, the presence of hydrogen containing groups, like hydroxyl groups in zeolite materials could promote this phenomenon [59].

As it was shown, the 1.0 wt. %Pd/HZSM-5/DeSi exhibited relatively high stability during three cycles of TCE HDC (Fig. 10). Only

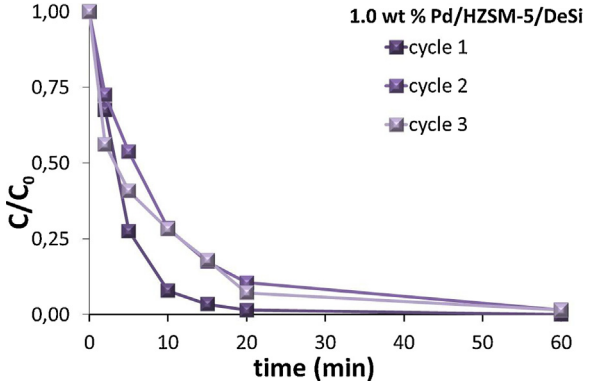

Fig. 10. Kinetics of HDC TCE on 1.0 wt.% Pd/HZSM-5/DeSi with subsequent reuse.

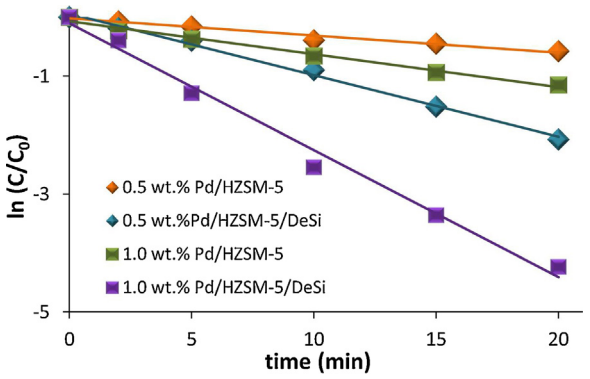

Fig. 11. Plot of ln (C/C_0) versus reaction time for hydrodechlorination of TCE on palladium containing HZSM-5 and HZSM-5/DeSi.

negligible differences in TCE conversion obtained after 60 min of subsequent reactions could be related rather with the catalyst mass loss during filtration and drying between the cycles and formation of Pd^{2+} species than the deactivation by leaching or formation deposits on catalyst support.

The hydrodechlorination of trichloroethylene on palladium deposited on zeolites HZSM-5 and HZSM-5/DeSi were assumed to be pseudo-first-order due to the predominant amount of hydrogen compared to TCE. The Fig. 11 shows the kinetic data according the linearized pseudo-first- order rate equation so the reaction kinetic can be ascribed as $\ln(C/C_0) = -kt$, where k is the apparent first—order rate constant (s^{-1}), and t is the reaction time (s). The reaction rate constant k was calculated to be 0.029 min^{-1} and 0.058 min^{-1} for the reaction catalysed by 0.5 wt.% Pd/HZSM-5 and 1.0 wt. %Pd/HZSM-5 respectively and 0.10 min^{-1} and 0.21 min^{-1} for the reaction catalysed by 0.5 wt.%Pd/HZSM-5/DeSi and 1.0 wt.%Pd/HZSM-5/DeSi zeolites. The k value obtained for 1.0 wt.%Pd/HZSM-5/DeSi zeolite is two times higher than that obtained for 0.5 wt.%Pd supported on the same zeolite, and accordingly seven or four times higher than k values obtained for two palladium loaded HZSM-5. Additionally, for quantitative comparison of catalysts activity, the amounts of palladium active sites were taken into account. Inspired by Dong et al. [55,56] we calculated the reaction rate constant with the consideration of the amounts of palladium species on catalyst surface $k_{Pd} = k/m_{Pd}$ (m_{Pd} – means weight of Pd active sites) too. They were determined as: 954.5 $min^{-1}\,g^{-1}$ for 1.0 wt.%Pd/HZSM-5/DeSi, 714.8 $min^{-1}\,g^{-1}$ for 0.5 wt.%Pd/HZSM-5/DeSi, 351.5 $min^{-1}\,g^{-1}$ for 1.0 wt.%Pd/HZSM-5 and 313.5 for 0.5 wt.% Pd/HZSM-5 $min^{-1}g^{-1}$, respectively. These values confirm the important role of the dispersion of metallic phase on hydrodechlorination process.

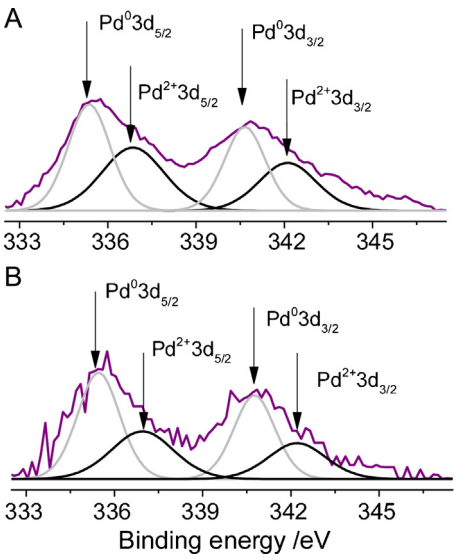

Fig. 12. XPS spectra of 1.0 wt.%Pd/HZSM-5/DeSi as synthetized (A) and (B) after the HDC of TCE reaction.

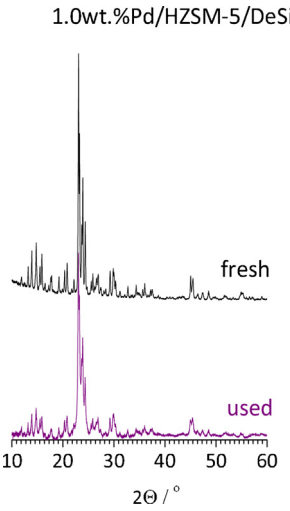

Fig. 13. XRD patterns of 1.0 wt.%Pd/HZSM-5/DeSi as synthetized and after the HDC of TCE reaction.

On the other hand TOF values calculated according to earlier studies of Molina et. al [54] showed the highest value for the catalyst with the highest dispersion of palladium supported on desilicated zeolite—0.5 wt.%Pd/HZSM-5/DeSi (Table 5). On the other hand, higher TOF value obtained for 0.5 wt.%Pd/HZSM-5 than for 1.0 wt.%Pd/HZSM-5 both with similar palladium dispersion confirm our supposition that catalytic properties of these materials depends on the presence of Brønsted and Lewis acid sites and their textural properties, too. Furthermore, the comparison of the activity of palladium loaded zeolites with other palladium catalysts in hydrodechlorination of trichloroethylene in aqueous phase clearly showed, that catalytic properties of Pd/HZSM-5 and Pd/HZSM-5/DeSi are better or comparable to the activity of CeO_2, activated carbons and graphite supported Pd [51,60] or CMC-stabilized palladium nanoparticles [61].

The water portions analysed by XRF after reaction did not show any amounts of palladium within the limits of the detection. Therefore, the effect of palladium leaching from the catalysts to reaction mixture in the case of 0.5 wt.%Pd/HZSM-5/DeSi and 1.0 wt.%Pd/HZSM-5/DeSi is believed to be negligible. Carbon bal-

ance has been estimated >90% for all reactions on palladium loaded zeolites.

The speciation of Pd in 1.0 wt.%Pd/HZSM-5/DeSi after HDC reaction was evaluated with X-ray photoelectron spectroscopy. The decomposition of the XPS (Fig. 12) spectrum at binding energies corresponding to Pd shows the presence of two peaks at 335.5 and 340.8 eV corresponding to Pd in its metallic state and other two peaks at 337.1 eV and 342.2 eV attributed to Pd in its oxidized state. The relative contribution of Pd^{2+} species was reduced in the catalyst after reaction (Fig. 12 B). Among the possible Pd^{2+} forms, i.e., PdO_x and $PdCl_x$, the palladium chloride species $PdCl_x$ are believed to dominate. However, no reflections in XRD patterns characteristic of palladium species were detected for the used catalysts (Fig. 13) pointing to their high dispersion preserved after reaction cycles and/or their amorphous nature.

4. Conclusions

The studies have shown that Pd-zeolite catalysts with the secondary mesopore system are very promising catalysts for the removal of TCE from water. It has been shown that catalytic performance of palladium loaded zeolite materials depends on their acidic and textural properties that influenced both noble metal dispersion and Pd^0/Pd^{2+} ratio. Palladium species uniformly dispersed on hierarchical zeolite HZSM-5/DeSi and taking the Pd^0 form predominantly were found to be significantly active in TCE HDC.

Acknowledgments

This work was financed by Grant No. 2013/09/B/ST5/00066 from the National Science Centre, Poland. The STEM studies were realized within the frame of the project “Infrastructure Improving of Centre of Excellence of Advanced Materials with Nano- and Submicron- Structure”, which is supported by the operational Program “Research and Development” financed through European Regional Development Fund. A.S.wt would like to thank National Science Centre for financial support within Grant No 2011/03/D/ST5/05516.

References

[1] B. Huang, Ch. Lei, Ch. Wei, G. Zeng, Environ. Int. 71 (2014) 118–138.
[2] M.J. Farre, S. Brosillon, X. Domenech, J. Peral, J. Photochem. Photobiol. A Chem. 189 (2007) 364–373.
[3] S. Giacomazzi, N. Cochet, Chemosphere 56 (2004) 1021–1168.
[4] E.D. Goldberg, Sci. Total Environ. 100 (1991) 17–28.
[5] V.I. Simagina, O.V. Netskina, E.S. Tayban, O.V. Komova, E.D. Grayfer, A.V. Ischenko, E.M. Pazhetnov, Appl. Catal. A General 379 (2010) 87–94.
[6] L. Calvo, M.A. Gilarranz, J.A. Casas, A.F. Mohedano, J.J. Rodriguez, Chem. Eng. J. 163 (2010) 212–220.
[7] M. Bonarowska, Z. Kaszkur, D. Łomot, M. Rawski, Z. Karpiński, Appl. Catal. B Environ. 162 (2015) 45–56.
[8] E. Diaz, A.F. Mohedano, J.A. Casas, L. Calvo, M.A. Gilarranz, J.J. Rodriguez, Catal. Today 241 (2015) 86–91.
[9] M. Martin-Martinez, A. Álvarez-Montero, L.M. Gómez-Sainero, R.T. Baker, J. Palomar, S. Omar, S. Eser, J.J. Rodriguez, Appl. Catal. B Environ. 162 (2015) 532–543.
[10] M. Al Bahri, L. Calvo, A.M. Polo, M.A. Gilarranz, A.F. Mohedano, J.J. Rodriguez, Chemosphere 91 (2013) 1317–1323.
[11] X. Le, Z. Dong, X. Li, W. Zhang, M. Le, J. Ma, Catal. Commun. 59 (2015) 21–25.
[12] I.A. Witońska, M.J. Walock, M. Binczarski, M. Lesiak, A.V. Stanishevsky, S. Karski, J. Mol. Catal. A Chemical 393 (2014) 248–256.
[13] E. Díaz, A. McCall, L. Faba, H. Sastre, S. Ordonez, Environ. Prog. Sustainable Energy 32 (2013) 1217–1222.
[14] S. Ordóñez, B.P. Vivas, F.V. Díez, Appl. Catal. B Environ. 195 (2010) 288–296.
[15] A. Elola, E. Díaz, S. Ordoñez, Environ. Sci. Technol. 43 (2009) 1999–2004.
[16] K. Tarach, K. Góra-Marek, J. Tekla, K. Brylewska, J. Datka, K. Mlekodaj, W. Makowski, M.C. Igualada López, J. Martínez Triguero, F. Rey, J. Catal. 312 (2014) 46–57.
[17] J. Jung, Ch. Jo, F.M. Mota, J. Cho, R. Ryoo, Appl. Catal. A Gen. 492 (2015) 68–75.
[18] B. Qin, X. Gao, F. Lin, B. Wang, Ch. Xu, J. Catal. 278 (2011) 266–275.
[19] Ch. Balsiger, Ch. Holliger, P. Hohener, Chemosphere 61 (2005) 361–373.
[20] A. Śrębowata, R. Baran, D. Łomot, D. Lisovytskiy, T. Onfroy, S. Dzwigaj, Appl. Catal. B Environ. 147 (2014) 208–220.
[21] A. Śrębowata, R. Baran, D. Lisovytskiy, I.I. Kamińska, S. Dzwigaj, Catal. Commun. 57 (2014) 107–110.
[22] J.M. Müller, G.C. Mesquita, S.M. Franco, L.D. Borges, J.L. de Macedo, J.A. Dias, S.C.L. Dias, Micropor. Mesopor. Mater. 204 (2015) 50–57.
[23] D. Verboekend, J. Pérez-Ramírez, Catal. Sci. Technol. 1 (2011) 879–890.
[24] Y. Tao, H. Kanoh, L. Abrams, K. Kaneko, Chem. Rev. 106 (2006) 896–910.
[25] J.C. Groen, J.C. Jansen, J.A. Moulijn, J. Pérez-Ramírez, J. Phys. Chem. B 108 (2004) 13062–13065.
[26] K. Sadowska, K. Góra-Marek, J. Datka, Vib. Spectrosc. 63 (2012) 418–425.
[27] K. Sadowska, K. Góra-Marek, M. Drozdek, P. Kuśtrowski, J. Datka, J. Martinez Triguero, F. Rey, Micropor. Mesopor. Mater. 168 (2013) 195–205.
[28] M. Hasik, A. Bernasik, A. Drelinkiewicz, K. Kowalski, E. Wenda, J. Camra, Surf. Sci. 507–510 (2002) 916–921.
[29] M. Hasik, A. Drelinkiewicz, M. Choczyński, S. Quilard, A. Proń, Synth. Met. 84 (1997) 93–100.
[30] J. Rouquerol, P. Llewellyn, F. Rouquerol, Stud. Surf. Sci. Catal. 160 (2007) 49–56.
[31] J. Huang, C.J. Xue, B.F. Wang, X.Z. Guo, S.R. Wang, React. Kinet. Mech. Catal. 108 (2013) 403–416.
[32] K. Okumura, S. Matsumoto, N. Nishiaki, M. Niwa, Appl. Catal. B Environ. 40 (2003) 151–159.
[33] K. Muto, N. Katada, M. Niwa, Appl. Catal. B Environ. 134 (1996) 203–215.
[34] J.A. Lercher, C. Gründling, G. Eder-Mirth, Catal. Today 27 (3–4) (1996) 353–376.
[35] K. Sadowska, K. Góra-Marek, J. Datka, Vibr. Spectrosc. 63 (2012) 418–425.
[36] M. Niwa, N. Katada, K. Okumura, Characterization and Design of Zeolite Catalysts: Solid Acidity, Shapeselectivity and Loading Properties, in: R. Hull, C. Jagadish, R.M. Osgood Jr., J. Parisi (Eds.), Springer Series of Material Science 141, 2015.
[37] M. Primet, L.C. De Menorval, J. Fraissard, T. Ito, J. Chem. Soc. Faraday Trans. 11 (1985) 2867–2874.
[38] Y. Yu, O.Y. Gutiérrez, G.L. Haller, R. Colby, B. Kabius, J.A. Rob van Veen, A. Jentys, J.A. Lercher, J. Catal. 304 (2013) 135–148.
[39] T. Rades, V.Y. Borokov, V.B. Kazansky, M. Polisset-Thfoin, J. Fraissard, J. Phys. Chem. 100 (1996) 16238–16241.
[40] S. Bertarione, C. Prestipino, E. Groppo, D. Scarano, G. Spoto, A. Zecchina, R. Pellegrini, G. Leofanti, C. Lamberti, Phys, Chem. Chem. Phys. 8 (2006) 3676–3681.
[41] E. Ozensoy, D.W. Goodman, Phys. Chem. Chem. Phys. 6 (2004) 3765–3778.
[42] G.V. Lowry, M. Reinhard, Environ. Sci. Technol. 34 (2000) 3217–3223.
[43] B. Schrick, J.L. Blough, A.D. Jones, T.E. Mallouk, Chem. Mater. 14 (12) (2002) 5140–5147.
[44] S. Doniacht, M. Sunjic, J. Phys. C Solid State Phys. 3 (1970) 285–291.
[45] K.S. Kim, A.F. Gossmann, N. Winograd, Anal. Chem. 46 (1975) 197–200.
[46] L.S. Kibis, A.I. Titkov, A.I. Stadnichenko, S.V. Koscheev, A.I. Boronin, Appl. Surf. Sci. 255 (2009) 248–9254.
[47] S. Wang, Y. Peng, Chem. Eng. J. 156 (2010) 11–24.
[48] W. Juszczyk, A. Malinowski, Z. Karpiński, Appl. Catal. A Gen. 166 (1998) 311–319.
[49] M.A. Aramendía, V. Boráu, I.M. García, C. Jiménez, F. Lafont, A. Marinas, J.M. Marinas, F.J. Urbano, J. Catal. 187 (1999) 392–399.
[50] J.A. Baeza, L. Calvo, M.A. Gilarranz, A.F. Mohedano, J.A. Casas, J.J. Rodriguez, J Catal. 293 (2012) 85–93.
[51] E. Díaz, L. Faba, S. Ordóñez, Appl. Catal. B 104 (2011) 415–417.
[52] T. Janiak, J. Okal, Appl. Catal B 92 (2009), 484–392.
[53] Y. Ren, G. Fan, Ch. Wang, J. Hazard. Mater. 274 (2014) 32–40.
[54] C.B. Molina, A.H. Pizarro, J.A. Casas, J.J. Rodriguez, Appl. Catal. B Environ. 148–149 (2014) 330–338.
[55] Z. Dong, X. Le, Y. Liu, Ch. Dong, J. Mater. Chem. A 2 (2014) 18775–18785.
[56] Z. Dong, X. Le, Ch. Dong, W. Zhang, X. Li, J. Mater. Appl. Catal. B Environ. 162 (2015) 372–380.
[57] S. Gómez-Quero, F. Cárdenas-Lizana, M.A. Keane, Ind. Eng. Chem. Res. 47 (2008) 6841–6853.
[58] S. Ordóñez, E. Díaz, R.F. Bueres, E. Asedegbega-Nieto, H. Sastre, J. Catal. 272 (2010) 158–168.
[59] D. Scarano, S. Bordiga, C. Lamberti, G. Ricchiardi, S. Bertarione, G. Spoto, Appl. Catal. A Gen. 307 (2006) 3–12.
[60] M. Cobo, J. Becerra, M. Castelblanco, B. Cifuentes, J.A. Conesa, J. Environ. Manage. 158 (2015) 1–10.
[61] M. Zhang, D.B. Bacik, Ch.B. Roberts, D. Zhao, Water Res. 47 (2013) 3706–3715.